Linear and Nonlinear Impairments when Adding and Dropping Superchannels in an Elastic Optical Network

Takuya Nakagawa, Yutaka Mori, Koichi Maru, Haruna Matsushita, and Masahiko Jinno
Kagawa University
2217-20 Hayashi-cho, Takamatsu, Kagawa 761-0396 Japan
jinno@eng.kagawa-u.ac.jp

***Abstract*— We investigate through simulation simultaneous linear and nonlinear impairments using a realistic reconfigurable optical add drop multiplexer (ROADM) model while considering optical filtering and in-band coherent crosstalk at each ROADM and the nonlinear interfering effects from neighbor superchannels with the QPSK or 16QAM modulation format.**

Keywords*— *elastic optical network; superchannel; frequency clipping; crosstalk; nonlinear impairment; Nyquist WDM

I. INTRODUCTION

The concept behind the elastic optical network (EON), *i.e.*, introducing elasticity and adaptation into the optical network, was reported and experimentally demonstrated in 2008 [1]. Since then, considerable research efforts have been dedicated toward exploring the potential of enhancing the efficiency of resource utilization and operational flexibility [2, 3] in optical networks. Due to its capability to generate various rate superchannels in a spectrum efficient manner, Nyquist wavelength division multiplexing (WDM) is gaining considerable interest as a key enabler for EONs [2]. Nyquist WDM is a multicarrier multiplexing scheme in which spectrally shaped subchannels are multiplexed in the optical domain with a bandwidth and frequency spacing that are both close to the symbol rate, R_s.

Extensive simulation, analytical, and experimental investigations of Nyquist-WDM superchannels over an uncompensated point-to-point coherent transmission system have been conducted [4, 5]. Since a wide variety of Nyquist-WDM superchannels with various bandwidths and modulation formats are added, routed, and dropped in EONs, it is very important to clarify how the adding and dropping of superchannels affects the transmission performance.

Recently, members of our research group showed through numerical simulations that reiterated adding/dropping of adjacent amplitude-varying 16QAM superchannels deteriorates the nonlinear transmission performance of co-propagated, long reach QPSK channels due to the non-negligible cross phase modulation (XPM) effect [6]. In addition, a high Q-factor was obtained for short add/drop intervals of co-propagated nonlinear-interfering superchannels. This nonlinear benefit from adding and dropping was experimentally demonstrated using a 120-Gb/s recirculating loop system [7].

This study was supported in part by JSPS KAKENHI grant Number 26220905 and the National Institute of Information and Communication Technology (NICT) under the R&D of Elastic Optical Networking Technologies.

In the previous paper, the ideal optical node with a lossless rectangular pass-band and an infinite blocking ratio were assumed in order to highlight the effect of nonlinear-interference in the fiber links [6]. In this paper, we report the results of an investigation based on simulation of linear and nonlinear impairments using a realistic reconfigurable optical add drop multiplexer (ROADM) model, considering optical filtering and in-band coherent crosstalk at each ROADM and the nonlinear interfering effects from neighbor superchannels with the QPSK or 16QAM modulation format.

II. SIMULATION CONDITIONS

A. ROADM and Link Models

Fig. 1 shows the ROADM model used in the simulation, which employs a broadcast and select architecture. The ROADM comprises splitters, monitor taps, and wavelength selective switches (WSSs), with the insertion losses of 10 dB, 1 dB, and 7 dB, respectively. The total loss of 20 dB is compensated by an optical amplifier with a 20-dB gain and 7-dB noise figure (NF).

Table I gives the link models used in the simulation. As transmission fibers, we consider a standard single mode fiber (SMF) with the dispersion coefficient of 18 ps/nm/km and effective core area of 80 μm^2, and a dispersion shifted fiber (DSF) with the dispersion coefficient of 2 ps/nm/km and

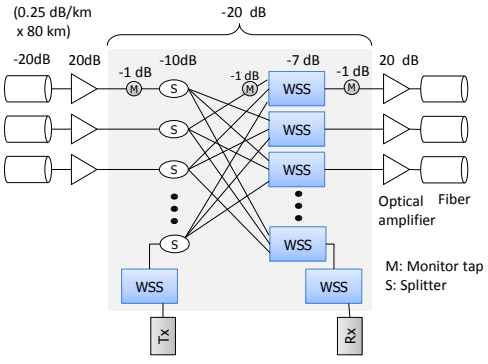

Fig. 1. ROADM model used in the simulation.

TABLE I. LINK MODELS USED IN THE SIMULATION

	SMF	DSF
Loss (dB/km)	0.22	
Fiber length (km)	80	
Total span loss (dB)	20	
Amplifier gain (dB)	20	
Noise figure (dB)	7	
Effective core area (micron^2)	80	50
Nonlinear index (m^2/W)	2.6×10^{-20}	
Dispersion (ps/nm/km)	18	2
Dispersion slope (ps/nm^2/km)	0.08	

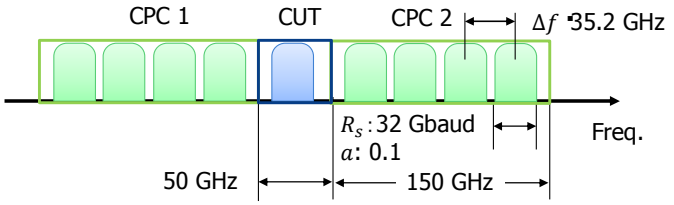

Fig. 2. Superchannel spectrum allocation used in the simulation. CUT: Channel under test, CPC: Co-propagating channel.

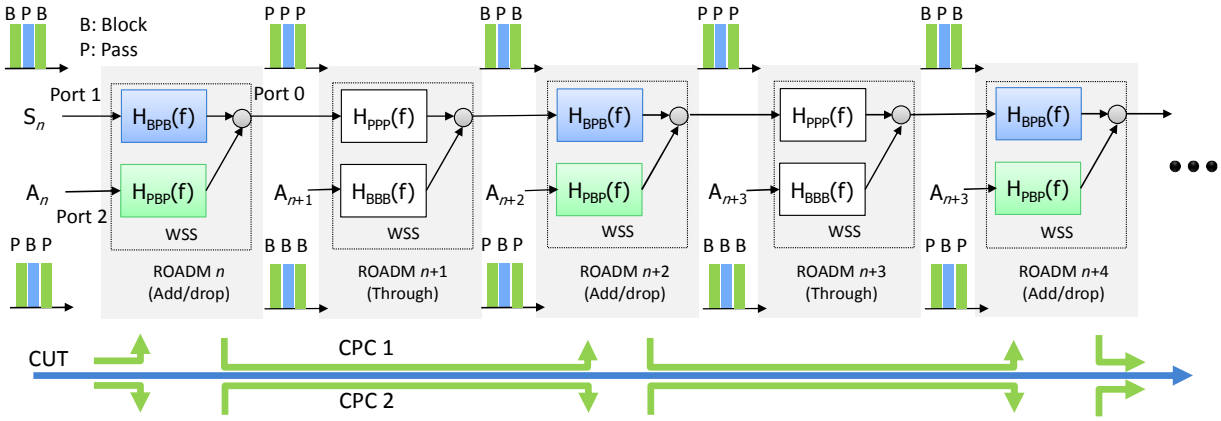

Fig. 3. Network model with WSS transfer functions: Co-propagating channels (CPCs) are add and dropped every 2 spans in this case.

effective core area of 50 μm^2. An in-line optical amplifier with a 20-dB gain and 7-dB NF is used to compensate for the total span loss of an 80 km fiber link.

B. *Superchannel Model*

The layout of the superchannels used in the simulation is the same as that used in [6] (See Fig. 2). In order to examine an extreme case, we arranged two co-propagating channels (CPCs) comprising four subcarriers at both sides of a channel under test (CUT) that comprises one spectrum-shaped subcarrier. Each subcarrier was coded with different pseudo random bit sequences and spectrally shaped by an electrical raised-cosine filter with a roll-off factor, α, of 0.1. The symbol rate, R_S, is 32 Gbaud, the frequency spacing, Δf, between each subcarrier is set to 35.2 GHz (= $R_s(1+\alpha)$), and the resulting assembled bandwidth for the CPCs is 140.8 GHz. The frequency slot widths allocated to the CPC and CUT are chosen to be 150 GHz and 50 GHz, respectively, in order to ensure sufficient guard-bands between them for routing, which coincides with the ITU-T flexible grid standard.

We tested two different modulation formats for the CPCs: NRZ-QPSK and NRZ-16QAM. If we assume polarization multiplexed QPSK for the CUT and CPCs, the simulation

layout corresponds to co-propagating two 400-Gb/s superchannels and one 100-Gb/s channel each having an optical transport network (OTN) overhead, a payload, and 20% FEC parity bits. Due to the limited implementation of digital signal processing algorithms in our simulation, we did not employ polarization division multiplexing and inserted an ideal dispersion compensation fiber with no loss and no nonlinear coefficient in front of the coherent receiver instead of applying electrical dispersion compensation.

C. *Network Model*

Fig. 3 shows the network model used in the simulation, in which ROADMs are cascaded to route superchannels and two CPCs are added and dropped at every 2 ROADMs for example. At ROADM n, the input signal, S_n, comprising the CUT and CPCs is launched into port 1 of WSS n that has the power transfer function of H_{BPB} (f), where the CPCs are blocked and the CUT experiences optical filtering. On the other hand, the add signal, A_n, comprising the potential in-band crosstalk signal with the same frequency as the CUT and CPCs, is launched into port 2 with the power transfer function of H_{PBP} (f), where the linear crosstalk signal is blocked and the CPCs are added. The resulting frequency-clipped CUT, imperfectly blocked in-band crosstalk signal, and the CPCs are then combined and propagated to the next ROADM n+1. Since the next ROADN n+1 is a through ROADM, we assume that the power transfer function of port 1, H_{PPP} (f), is flat over the frequency slot of the CUT, meaning that no optical filtering occurs. Similarly, we assume the power transfer function of port 2, H_{BBB} (f), is sufficiently low to block perfectly the linear crosstalk signal.

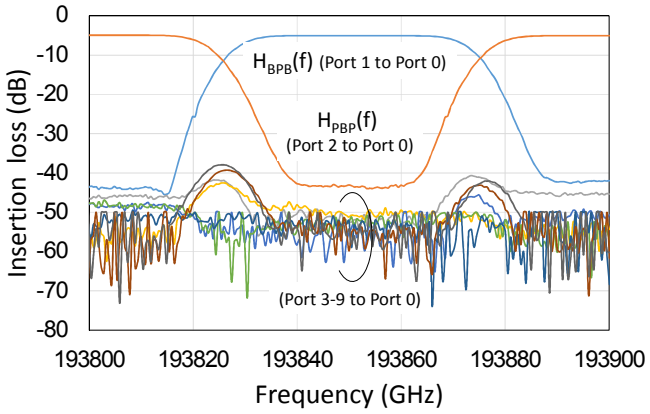

Fig. 4. Insertion losses of WSS used in the simulation for the pass band width set to 50 GHz (0.5-dB bandwidth: 35.6 GHz, 3-dB bandwidth: 44.6 GHz).

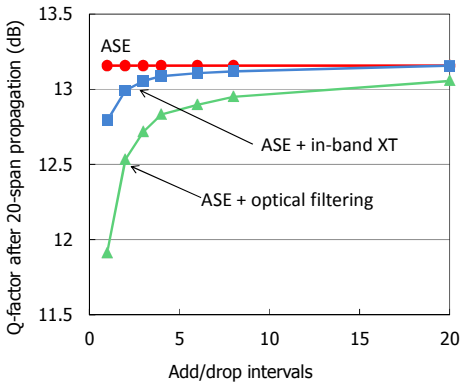

Fig. 5. Q-factor after the 20-span propagation of 32-Gbaud QPSK signal calculated when the effects of (1) ASE noise alone, (2) ASE and in-band crosstalk, and (3) ASE and optical filtering are included.

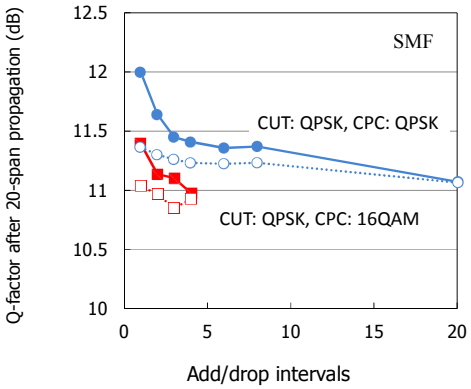

Fig. 6. Q-factor after the 20-span propagation of 32-Gbaud QPSK signal calculated when ASE and nonlinear effects for SMF are included (other linear impairments are excluded). Open plots indicate results when CPSs are pre-dispersed.

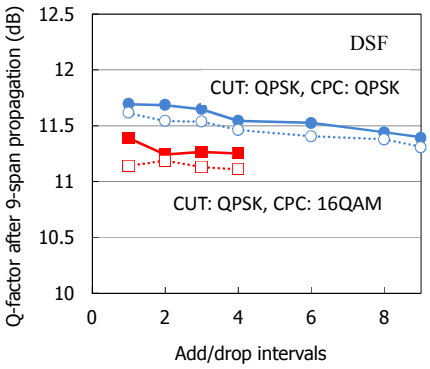

Fig. 7. Q-factor after the 9-span propagation of 32-Gbaud QPSK signal calculated when ASE and nonlinear effects for DSF are included (other linear impairments are excluded). Open plots indicate results when CPSs are pre-dispersed.

Fig. 4 shows H_{BPB} (f) and H_{PBP} (f) used in the simulation, which are obtained with a commercially available 1 × 9 WSS when the slot width for the CUT is set to 50 GHz. The 0.5-dB and 3-dB bandwidths are 35.6 GHz and 44.6 GHz, respectively. The blocking ratio measured at the center of the stop band is 38.4 dB.

III. Simulation Results

A. Linear Impairments

In order to identify the breakdown of linear and nonlinear impairments in the transmission performance in an EON, we first investigate the linear contribution by using the ROADM and link models described in the previous section but set the fiber nonlinear index to zero. Fig. 5 shows the Q-factors after 20-span propagation as a function of the add/drop intervals ranging from every span to every eight spans. Simulations are performed for three cases: including the effect(s) of (1) amplified spontaneous emission (ASE) accumulated alone as a baseline, (2) ASE accumulation and in-band coherent crosstalk generated through an imperfect stopband, and (3) ASE accumulation and optical filtering caused by a non-rectangular passband. As expected, the Q-factors for (2) and (3) degrade inversely proportionally to the add/drop interval. The slight decrease in the Q-factor observed at the add/drop interval of 20 is due to the passing of a WSS at the source and destination ROADMs.

B. Nonlinear Effects

Next, we investigate the nonlinear impairments by using the ROADM and link models described in the previous section. The linear impairments are excluded by replacing the measured power transfer functions of the WSS with the ideal rectangular filter with a 7-dB insertion loss. In Fig. 6, the Q-penalty for the SMF measured after 20 spans as a function of the add/drop intervals, is plotted with solid lines and closed plots for the following cases: (1) QPSK is employed for both CUT and CPCs (indicated by blue circles), and (2) QPSK and 16QAM are employed for CUT and CPCs (indicated by red squares). Note that since the optical reach for 16QAM CPCs is much shorter than that of the QPSK CUT and the maximum add/drop intervals is limited to 4 spans, 16QAM CPCs can interfere along the entire length of a longer optical-reach QPSK CUT, by adding new 16QAM CPCs one-after- another. In order to

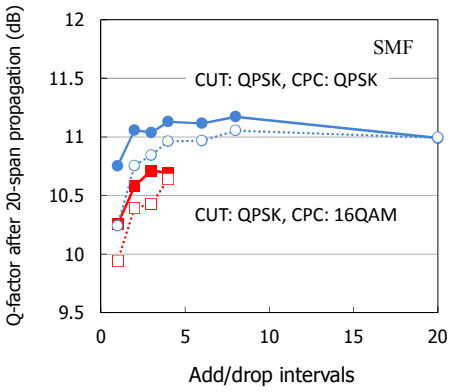

Fig. 8. Q-factor propagation of 32-Gbaud QPSK signal after the 20-span of SMF calculated when all impairment factors are included. Open plots indicate results when CPSs are pre-dispersed.

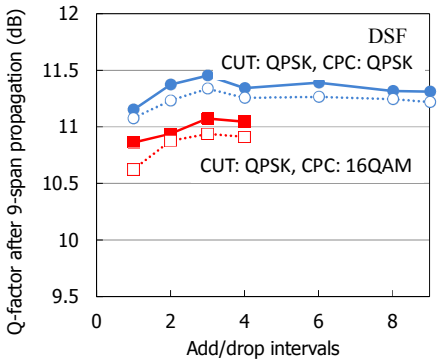

Fig. 9. Q-factor propagation of 32-Gbaud QPSK signal after the 9-span of DSF calculated when all impairment factors are included. Open plots indicate results when CPSs are pre-dispersed.

investigate the effect of pre-dispersion of the CPCs [7] in detail, we performed the same simulation but applied the chromatic dispersion of 1440 ps/nm (corresponding to one-span transmission of the SMF) to the CPCs before adding them at each ROADM. The results are also shown in Fig. 6 as dotted lines and open plots. From the figure, we observe the following.

(i) 16QAM yields more severe impairment than QPSK. This is due to the larger amplitude variation of 16QAM.

(ii) The Q-factor improves as the add/drop interval decreases. This improvement is suppressed when the CPCs are pre-distorted.

Similar results are obtained for the DSF with a rather lower degree of improvement in the Q-factor and lower level of suppression for the pre-dispersion as shown in Fig. 7. This can be understood as follows. The peak-to-average power ratio (PAPR) of the NRZ signal increases with the increase in the chromatic dispersion that the signal experiences and becomes saturated for chromatic dispersion greater than ~1000 ps/nm [8]. This means that for the SMF the PAPR of the signal reaches its saturation point at the end of the first span. Since a higher PAPR causes stronger nonlinear impairments, the presence or absence of the initial distortion strongly affects the Q-factor performance for the SMF. On the other hand, since the level of chromatic dispersion in the DSF is approximately 10 times lower than that in the SMF, the PAPR of the signal gradually increases with the span, and improvement in the Q-factor and dependence of the initial distortion are rather moderate.

C. *Total Performance*

Figs. 8 and 9 show the Q-factors for the SMF and DSF, respectively, as a function of the add/drop interval when all the contributions are included. For both cases, the worst Q-factor is obtained when the add/drop interval is 1, reflecting the fact that the optical filtering effect is dominant under our simulation conditions.

IV. Conclusions

We reported detailed results of a simulation-based investigation on linear and nonlinear impairments using a realistic ROADM and link models. The simulations considered optical filtering and in-band coherent crosstalk at each ROADM and nonlinear interfering effects from neighbor superchannels with the QPSK or 16QAM modulation format. We showed that the frequent adding and dropping mitigates the nonlinear impairment but strengthens the optical filtering and the in-band coherent crosstalk effects. The latter linear impairments are the dominant factor under our simulation conditions. As a result, the total Q-factor performance is degraded as the add/drop interval decreases.

References

[1] M. Jinno, *et al.*, "Demonstration of novel spectrum-efficient elastic optical path network with per-channel variable capacity of 40 Gb/s to over 400 Gb/s," Proc. ECOC 2008, Th3F6, 2008.

[2] O. Gerstel, M. Jinno, A. Lord, and S. J. B. Yoo, "Elastic optical networking: A new dawn for the optical layer?," IEEE Commun. Mag., 50, S12–S20, 2012.

[3] M. Jinno, H. Takara, and K. Yonenaga, "Virtualization in optical networks from network level to hardware level," J. Opt. Comm. and Netw., 5, A46–A56, 2013.

[4] A. Carena, V. Curri, G. Bosco, P. Poggiolini, and F. Forghieri, "Modeling of the impact of nonlinear propagation effects in uncompensated optical links," J. Lightwave Technol. 30, pp. 1524-1539, 2012.

[5] P. Poggolini, "The GN model of non-Linear propagation in uncompensated coherent optical systems," J. Lightwave Technol. 30, 24, pp. 3857-3879, 2012.

[6] M. Jinno, K. Hosokawa, S. Kuwahara, Y. Yamada, and T. Kataoka, "Impact of adding/dropping Nyquest WDM superchannels on transmission performance in an elastic optical network," Proc. OECC 2014, WE7A-3, 2014.

[7] S. Searcy and S. Tibuleac, "Impact of channel add/drop on nonlinear performance in uncompensated 100G coherent systems," Proc. OFC 2015, M3A.6, 2015.

[8] C. Xie, "Chromatic dispersion estimation for single-carrier coherent optical communications," IEEE Photon. Tecnol. Lett., 25, 10, pp. 992-995, 2013.